Cell

A Bacterial Effector Targets Mad2L2, an APC Inhibitor, to Modulate Host Cell Cycling

Hiroki Iwai,[1,7] Minsoo Kim,[1,7] Yuko Yoshikawa,[1] Hiroshi Ashida,[1] Michinaga Ogawa,[1] Yukihiro Fujita,[1] Daniel Muller,[1] Teruo Kirikae,[4] Peter K. Jackson,[5] Shuji Kotani,[3,8] and Chihiro Sasakawa[1,2,6,*]

[1]Department of Microbiology and Immunology
[2]Department of Infectious Disease Control
International Research Center for Infectious Diseases, Institute of Medical Science, University of Tokyo, 4-6-1, Shirokanedai, Minato-ku, Tokyo 108-8639, Japan
[3]Department of Molecular Cytogenetics, Medical Research Institute, Tokyo Medical and Dental University, 1-5-45, Yushima, Bunkyou-ku, Tokyo 113-0034, Japan
[4]Department of Infectious Diseases, Research Institute, International Medical Center of Japan, 1-21-1, Toyama, Shinjuku, Tokyo 162-8655, Japan
[5]Genentech, Inc., 1 DNA Way, South San Francisco, CA 94080, USA
[6]CREST, Japan Science and Technology Agency, Kawaguchi 332-0012, Japan
[7]These authors contributed equally to this work.
[8]Present address: Department of Internal Medicine, Arakawa Ryoyou Hospital, Arakawa, Tokyo, 116-0000, Japan
*Correspondence: sasakawa@ims.u-tokyo.ac.jp
DOI 10.1016/j.cell.2007.06.043

SUMMARY

The gut epithelium self-renews every several days, providing an important innate defense system that limits bacterial colonization. Nevertheless, many bacterial pathogens, including *Shigella,* efficiently colonize the intestinal epithelium. Here, we show that the *Shigella* effector IpaB, when delivered into epithelial cells, causes cell-cycle arrest by targeting Mad2L2, an anaphase-promoting complex/cyclosome (APC) inhibitor. Cyclin B1 ubiquitination assays revealed that APC undergoes unscheduled activation due to IpaB interaction with the APC inhibitor Mad2L2. Synchronized HeLa cells infected with *Shigella* failed to accumulate Cyclin B1, Cdc20, and Plk1, causing cell-cycle arrest at the G2/M phase in an IpaB/Mad2L2-dependent manner. IpaB/Mad2L2-dependent cell-cycle arrest by *Shigella* infection was also demonstrated in rabbit intestinal crypt progenitors, and the IpaB-mediated arrest contributed to efficient colonization of the host cells. These results strongly indicate that *Shigella* employ special tactics to influence epithelial renewal in order to promote bacterial colonization of intestinal epithelium.

INTRODUCTION

Shigella are highly adapted human pathogens that cause bacillary dysentery, a disease that provokes severely bloody and mucous-containing diarrhea. *Shigella* belong to the *Escherichia coli* family, but unlike other pathogenic *E. coli*, *Shigella* have no adherence factors. Thus, following ingestion via the fecal-oral route, *Shigella* reach the colon and rectum and translocate through the epithelial barrier via M cells overlying solitary lymphoid nodules. Once they pass through the M cells, *Shigella* infect the resident macrophages and escape from the macrophages' phagosomes into the cytoplasm, where they multiply and induce rapid cell death (Sansonetti, 2004; Ogawa and Sasakawa, 2006). *Shigella* released from dead macrophages enter the surrounding enterocytes through the basolateral surface by inducing macropinocytosis. After a bacterium is surrounded by the membrane vacuole of an epithelial cell, it disrupts the vacuolar membrane and escapes into the cytoplasm. *Shigella* multiply in the cytoplasm and move intra- and intercellularly by inducing actin polymerization at one pole of the bacterium; this polymerization is required for cell-cell spreading (Cossart and Sansonetti, 2004; Ogawa and Sasakawa, 2006).

While establishing colonization, *Shigella* deliver a variety of virulence determinants, and the major determinants, called effectors, are delivered through the type III secretion system (TTSS) into host cells. For example, after *Shigella* contact epithelial cells, the TTSS is stimulated and delivers effectors including IpaA, IpaB, IpaC, IpgB1, IpgD, and VirA into the host cells; these effectors promote bacterial invasion of host cells (Ogawa and Sasakawa, 2006; Parsot, 2005). One of these effectors, IpaB, plays multiple roles in promoting *Shigella* infection. The IpaB protein delivered into macrophages activates Caspase-1 and induces cell death (Hilbi et al., 1998, Chen et al., 1996; Zychlinsky et al., 1992). IpaB also interacts with CD44 on the epithelial cell membrane and stimulates

bacterial basolateral invasion (Lafont et al., 2002). Upon contact of *Shigella* with the host plasma membrane, IpaB, together with IpaC secreted at the tip of the TTSS needle, acts as a membrane-pore-forming protein, mediating the translocation of effectors via the TTSS into the host cell cytoplasm (Blocker et al., 1999). IpaB is also delivered into the epithelial intracellular compartment during *Shigella* infection, but its biological role there is unknown.

The intestinal epithelium self-renews every several days, providing an important intrinsic defense system that limits bacterial colonization (Oswald et al., 2005; Sansonetti, 2004). The fast turnover of intestinal epithelial cells forms crucial physical as well as functional barriers, and this renewal is sustained by vigorous proliferation of epithelial progenitors that migrate upwards from the bottom of the intestinal crypts (Potten, 1998). Indeed, lesions in the epithelial barrier are quickly repaired; if not, commensal and pathogenic bacteria can enter the wound. Nevertheless, many bacterial pathogens, including *Shigella*, are capable of colonizing the intestinal barriers. As mentioned above, *Shigella* (as well as many other mucosal Gram-negative pathogenic bacteria) have developed a variety of tactics to manipulate host cell functions in order to avoid or overcome the innate host defense system. Recent studies have indicated that a growing family of bacterial toxins and effectors, termed "cyclomodulins," interfere with the eukaryotic cell cycle, presumably to the pathogens' benefit (Oswald et al., 2005). Some of these cyclomodulins, such as the Cytolethal distending toxin (CDTs), are produced by a group of unrelated Gram-negative bacteria that includes *S. dysenteriae* (Nougayrede et al., 2005). One of the CDTs produced by *Campylobacter jejuni* possess a deoxyribonuclease I-like activity and causes limited DNA damage when delivered into a host cell nucleus, eventually leading to chromatin disruption (Lara-Tejero and Galan, 2000). Another cyclomodulin, Cycle inhibiting factor (Cif) inhibits host cell mitosis after transfer from enteropathogenic *E. coli* via the TTSS (Marches et al., 2003). Cells transformed by Cif accumulate 4n DNA content and reinitiate DNA synthesis without dividing, resulting in 8–16n DNA content. G2 arrest of the host cell cycle is associated with the maintenance of Cdk1, a cyclin-dependent kinase (Cdk), in its premitotic tyrosine-phosphorylated state (Marches et al., 2003). However, the mechanisms underlying Cif-mediated Cdk1 inactivation are unclear. Thus, some cell-cycle inhibitors are anticipated to help prolong the pathogen's presence by interfering with the rapid turnover of epithelial cells or by harming the local epithelial barrier, allowing the entry of pathogenic bacteria into the subepithelial layer (Lara-Tejero and Galan, 2002).

Cell-cycle progression is stringently controlled by cell-cycle-specific proteolysis that involves the ubiquitination of target proteins by two main types of E3 ligase complexes, the anaphase-promoting complex (APC) and the Skp1-Cullin-F-box protein (SCF) complex (Vodermaier, 2004). The APC is a multisubunit complex that targets substrates for degradation only during mitosis and G1, and it also targets mitotic Cyclin A and Cyclin B1, allowing mitotic progression. Two proteins, Cdc20 and Cdc20 homolog 1 (Cdh1), bind directly to APC and thereby activate APC during mitosis and in the late mitotic and G1 phases, respectively (Peters, 2002). Mad2 and the spindle assembly checkpoint pathway inhibit APC^{Cdc20} activity in response to spindle damage (Nasmyth, 2005), and Early mitotic inhibitor 1 (Emi1) inhibits both Cdc20 and Cdh1 in S and M phases (Hsu et al., 2002; Reimann et al., 2001a). However, additional APC regulators have been postulated to exist in order to ensure the destruction of APC substrates at the correct time and place. Indeed, recent studies have identified p31-comet as a Mad2-binding partner (Habu et al., 2002). In synchronized HeLa cells, Mad2 forms a complex with Cdc20 during prometaphase and metaphase; once the anaphase checkpoint is satisfied, the Mad2-Cdc20 complex is dissociated by the binding of Mad2 to p31-comet. Thus, p31-comet plays a critical role in relieving inhibition of the Cdc20-containing APC complex (Xia et al., 2004). Mad2L2, also referred to as Mad2B or hRev7 (Chen and Fang, 2001; Cheung et al., 2006; Pfleger et al., 2001) (Mad2L2 hereafter), which shares 25% amino acid identity and 48% amino acid similarity to Mad2, was recently suggested to control APC activation by Cdc20 (APC^{Cdc20}) and also to suppress APC activation by Cdh1 (APC^{Cdh1}) (Chen and Fang, 2001; Pfleger et al., 2001). Because Emi1 is capable of suppressing APC^{Cdh1} activation in human cell lines, it is assumed that Mad2L2's function is similar to that of Emi1 in controlling the APC activation required for the cell-cycle transition.

In this study we investigated the route of *Shigella* infection of the intestinal epithelium using rabbit ileal loops at various stages of infection and noted that *Shigella* are capable of accessing the intestinal crypt after inducing inflammatory responses in the intestinal tissue. We found that the bacterial infection also reduces the proliferation of epithelial progenitors, as shown by Proliferating cell nuclear antigen (PCNA) staining. The effect was absent following innoculation with a TTSS-deficient—and therefore noninvasive—*Shigella* mutant, such as the *ipaB* deletion mutant. More remarkably, we found that after transfer from *Shigella* into epithelial cells, intracellular IpaB can also be translocated into the host cell nucleus. This observation led us to further investigate the role of IpaB in *Shigella* infection of intestinal epithelial cells.

RESULTS

Shigella IpaB Targets Mad2L2 in Epithelial Cells at G2/M Phase

To explore the role of IpaB delivered into epithelial cells during *Shigella* infection of intestine, we performed yeast two-hybrid screening of HeLa cDNA library and found that IpaB interacted with Mad2L2, an APC inhibitor (Figure 1A). Under these conditions, IpaB was incapable of interacting with other APC inhibitors, such as Emi1 and Mad2 (Figure 1A). The IpaB/Mad2L2 interaction was

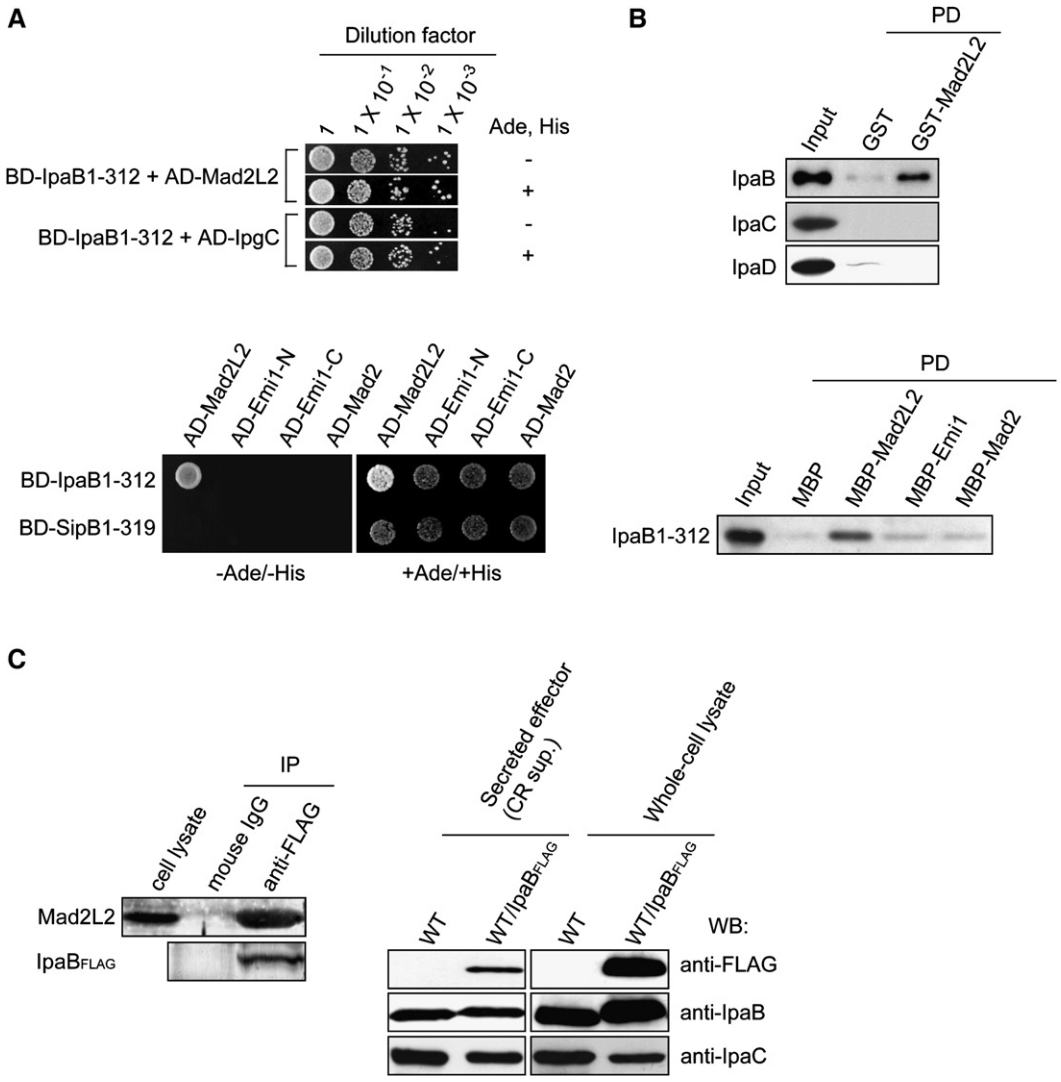

Figure 1. IpaB Interacts with Mad2L2

(A) Binding of BD-IpaB1-312, BD-SipB1-319, AD-Mad2L2, AD-IpgC, AD-Emi1-N1-300, AD-Emi1-C250-447, and AD-Mad2 in a yeast two-hybrid assay.

(B) IpaB bound to Mad2L2 in the GST-pull down assay (top). IpaB1-312 bound to MBP-Mad2L2 in the MBP pull-down assay but not to MBP-Emi1, MBP-Mad2, or MBP (bottom). Proteins that were pulled down were immunoblotted with antibodies specific for IpaB, IpaC, or IpaD.

(C) Cell lysates from HeLa cells infected with WT/$IpaB_{FLAG}$ were immunoprecipitated with anti-FLAG antibody or mouse IgG, and then immunoblotted with anti-Mad2L2 or -FLAG antibodies (left). Secretion of $IpaB_{FLAG}$ from *Shigella* was confirmed using Congo red (CR)-treated supernatants from WT or WT/$IpaB_{FLAG}$ in immunoblots with anti-IpaB, -IpaC, or -FLAG antibodies (right).

confirmed by GST and MBP pull-down assays (Figure 1B). To test the ability of IpaB to interact with endogenous Mad2L2 we infected HeLa cells with WT/$IpaB_{FLAG}$. This *Shigella* strain expressed $IpaB_{FLAG}$ from the endogenous 220 kb plasmid (Figure S1A) and carried Δ*dapB* so that intracellular *Shigella* would not kill the host cells in medium depleted of diaminopimelic acids (DAP). The expressed $IpaB_{FLAG}$ conferred wild-type TTSS activity (Figure 1C, right) and invasiveness (Figure S1B). In addition, the strain expressed AfaE (Afimbrial adhesin E) from *E. coli* to boost infection of HeLa cells (Philpott et al., 2000). Twenty-one hours after infection of asynchoronously dividing HeLa cells, the length of time normally required for a HeLa cell doubling, Mad2L2 was coimmunoprecipitated with $IpaB_{FLAG}$ (Figure 1C, left). We next investigated the intracellular locations of IpaB and Mad2L2 in HeLa cells expressing GFP-IpaB1-312/Myc_6-Mad2L2 or GFP-mock/Myc_6-Mad2L2 at the G1/S boundary induced by double thymidine block (DTB) (Figure 2) Myc_6-Mad2L2 and the GFP control were detected in the nucleus and cytoplasm from 0 to 15 hr. Although GFP-IpaB1-312 was detected in the cytoplasm by 3 hr after DTB, IpaB and Mad2L2 were

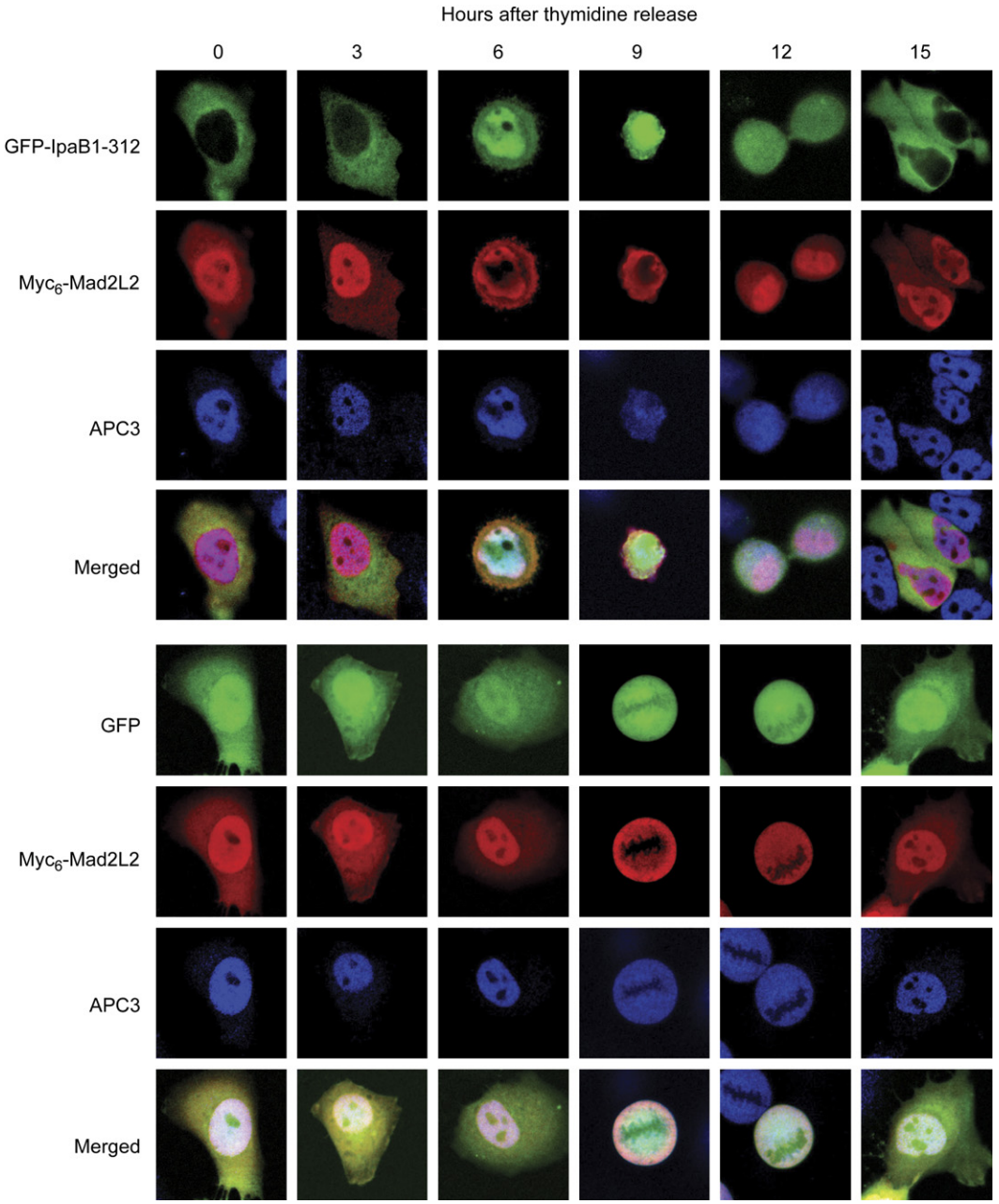

Figure 2. IpaB Localizes in the Nuclei of HeLa Cells during G2/M Phase

GFP-IpaB1-312 and Myc_6-Mad2L2 expressed in HeLa cells were visualized after G1/S release. HeLa-expressed GFP and Myc_6-Mad2L2 were similarly examined. Cells were stained with TRITC-labeled anti-Myc antibody and Cy5-labeled anti-APC3 antibody.

detected in the nucleus between 6 and 12 hr (Figure 2), suggesting that IpaB interacts with Mad2L2 in the G2/M phase.

Mad2, BubR1, Emi1, and RASSF1A are known APC inhibitors in humans (Fang et al., 1998; Hsu et al., 2002; Song et al., 2004; Tang et al., 2001). Since the ability of Mad2L2 to inhibit APC was previously determined only in *Xenopus* (Chen and Fang, 2001; Pfleger et al., 2001), we generated human anti-Mad2L2 antibody (Figure S2). When HeLa cell lysates were immunoprecipitated with anti-Mad2L2 or -Mad2 antibody, APC3, a component of APC, was coprecipitated (Figure S3A, upper and bottom). When HeLa cell lysates were immunoprecipitated with anti-APC3 antibody Emi1 was coprecipitated (Figure S3A, middle). To identify the cell-cycle phase involved in the Mad2L2/APC interaction, HeLa cells synchronized at the G1/S boundary were lysed at various times after DTB release and immunoprecipitated with anti-Mad2L2,

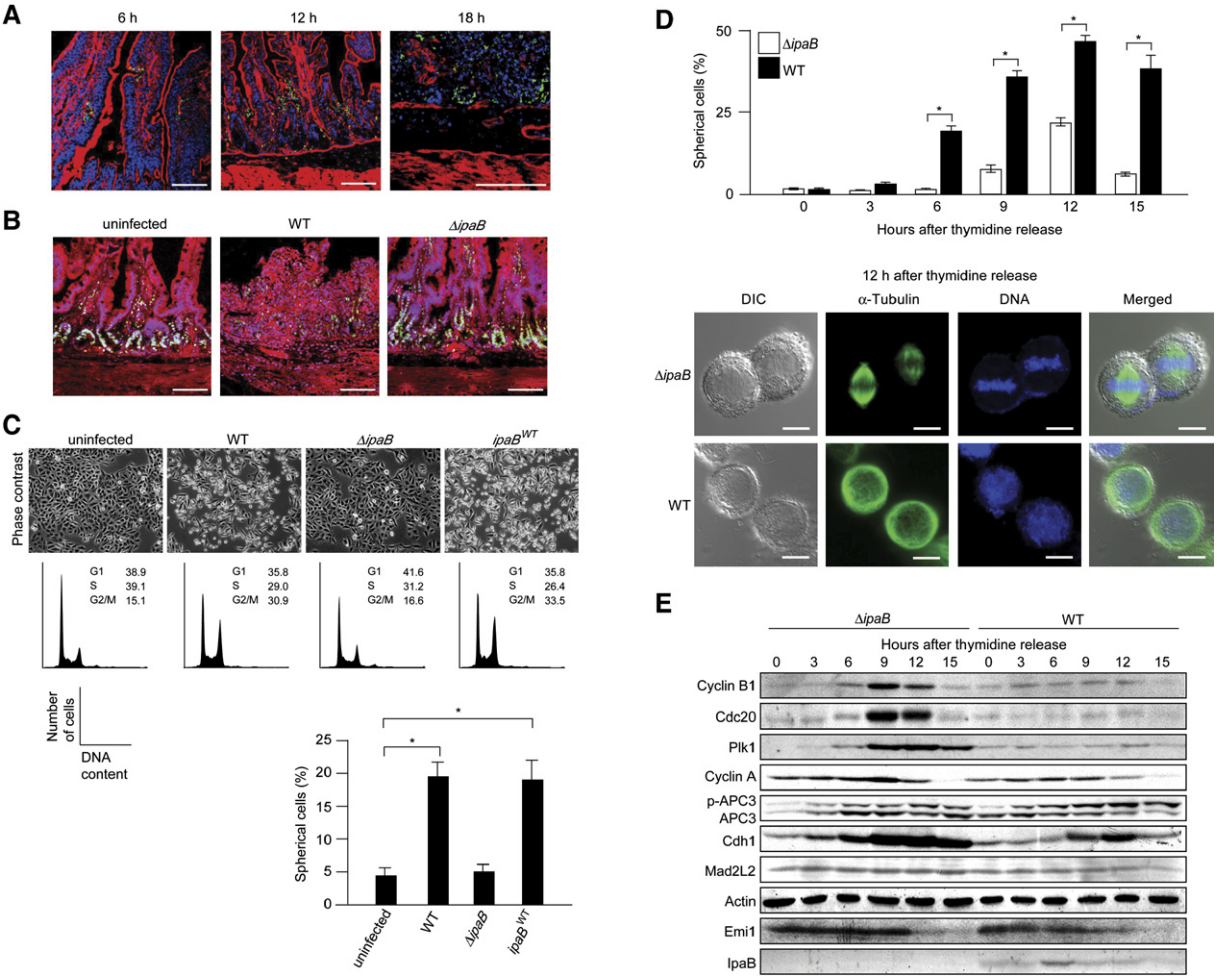

Figure 3. *Shigella* Cause Cell-Cycle Arrest

(A) Rabbit ileal loops 6, 12, and 18 hr after inoculation with 2 × 10^8 GFP-*Shigella* were stained with rhodamine-phalloidin (red) and TO-PRO3 (blue). Bars, 100 μm.

(B) The intestinal tissues were immunostained with FITC-labeled anti-PCNA antibody (green) and counterstained with rhodamine-phalloidin (red) and TO-PRO3 (blue). Bars, 100 μm.

(C) Spherical HeLa cells after infection with WT, Δ*ipaB*, or *ipaB*^{WT} (moi 80) (upper) and their percentages (bottom). *p < 0.0001. Data are represented as mean ± SEM. Cell-cycle stage distribution was determined by FACS (middle).

(D) Spherical cells among synchronized HeLa cells infected with Δ*ipaB* or WT (top). *p < 0.0001. Data are represented as mean ± SEM. HeLa spindle formation was impaired by WT infection but not by Δ*ipaB* infection. DIC, α-tubulin (green) and DNA (blue). Bars, 10 μm.

(E) Levels of cell-cycle-associated proteins in the cells used for (D) immunoblotting, with the specific antibodies indicated.

-APC3, or -Mad2 antibodies. The results showed that Mad2L2 interacted with APC primarily in G2/M phase (Figure S3B). The cell-cycle distribution was monitored by scoring the percentage of spherical cells (Figure S3C) and using FACS analysis of DNA content (Figure S3D).

Shigella Infection of Epithelial Cells Causes Unscheduled Activation of APC^{Cdh1}

To investigate whether *Shigella* affect the proliferation of intestinal epithelial progenitors, YSH6000 (WT/pSU-GFP) were visualized after inoculation into a rabbit ileal loop (Figure 3A). Twelve and eighteen hours after inoculation, WT/pSU-GFP was detected at the bottom of crypts. WT/pSU-GFP or the *ipaB* mutant (Δ*ipaB*/pSU-GFP) was inoculated into rabbit ileal loops, and intestinal tissue was examined 15 hr later. WT/pSU-GFP, but not Δ*ipaB*/pSU-GFP, destroyed the intestinal villi; on the other hand, PCNA-positive cells in the crypts in *Shigella*-infected loops were barely detected (Figure 3B), implying that *Shigella* interfer with the proliferation of epithelial progenitors. HeLa cells were infected with or without *dapB::*Km/pIL14-Tp (bacteria expressing AfaE) (WT) in the presence of DAP for 5 min. When HeLa cells cultured for 24 hr in DAP-free, gentamicin-containing MEM were infected with WT and *ipaB*^{WT}/*dapB::*Km/pIL14-Tp (*ipaB*^{WT}) (*ipaB* complement), approximately 20% of the infected

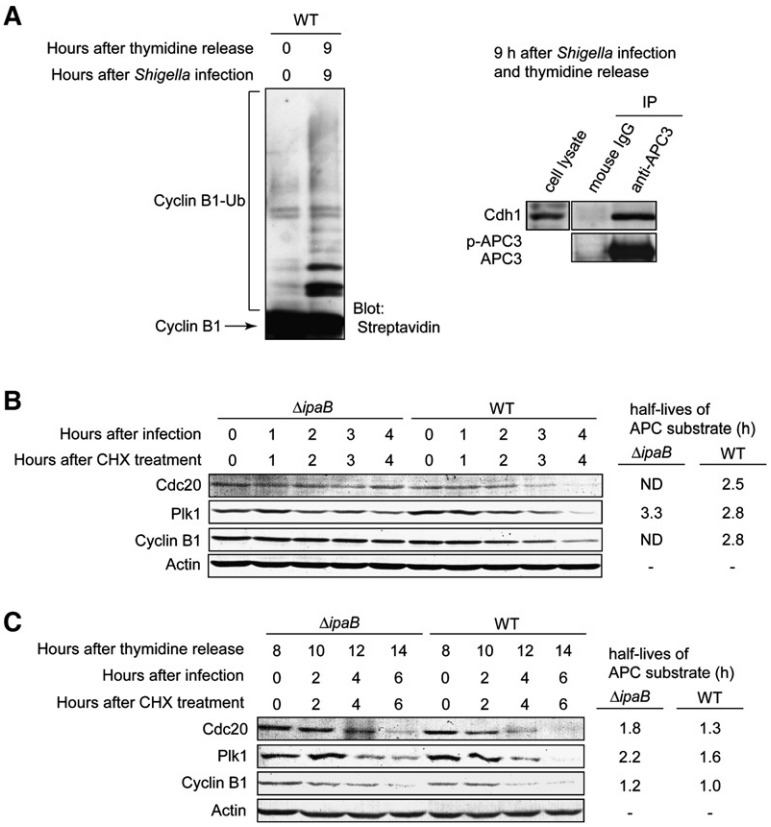

Figure 4. *Shigella* Cause Premature Activation of APC^{Cdh1}

(A) Analysis of Cyclin B1 ubiquitination activity in *Shigella*-infected HeLa cells. APC was immunopurified from HeLa cells infected with WT and then incubated with biotinylated Cyclin B1 and ubiquitin (Left). Control mouse IgG or anti-APC3 immunoprecipitates from HeLa cells infected with WT were immunoblotted with anti-Cdh1 or -APC3 antibodies (right).

(B) Effect of *Shigella ipaB* genotype on the half-lives of APC substrates after inoculation of asynchronous HeLa cells. Cychloheximide (CHX, 100 μg/ml) was added, and cell extracts were prepared at the time points indicated to investigate the half-lives of Cdc20, Plk1, Cyclin B1. ND indicates that changes in protein levels were not detected.

(C) Effect of WT or Δ*ipaB* infection of synchronous HeLa cells on the half-lives of the APC substrates.

cells, mostly those at G2/M phase, became spherical (Figure 3C) and TUNEL-negative (data not shown), indicating that *Shigella* infection interfers with cell-cycle progression. This was not the case with Δ*ipaB*/*dapB::*Km/pIL14-Tp (Δ*ipaB*) (Figure 3C). To characterize the spherical cells, DTB-synchronized cells at the G1/S boundary were infected with WT or Δ*ipaB*, and 5 min later the medium was replaced with DAP-free, gentamicin-containing MEM. WT infection resulted in more spherical cells than did Δ*ipaB* infection (Figure 3D, upper panel). Spherical cells with condensed chromatin emerged by 12 hr after infection with the WT bacteria (Figure 3D, lower panel), whereas the cells generated by Δ*ipaB* infection had the metaphase chromosome alignment and spindle organization (Figure 3D, lower panel).

Consistent with the results of Figure 2, spherical cells following WT infection were detected 6 hr after DTB release (Figure 3D), suggesting that *Shigella* infection led to M phase arrest. Immunoblotting of HeLa cells synchronized in G1/S phase showed that although Cyclin B1, Cdc20, and Plk1 accumulated approximately 9 hr after DTB release following Δ*ipaB* infection, they were abolished after WT infection (Figure 3E). WT infection was also followed by an increase in phosphorylated (active) APC, as well as a decrease in Cdh1 (an APC activator), compared with in the conditions following Δ*ipaB* infection. After WT infection, the accumulation of Cdc20 and Plk1, known substrates of APC^{Cdh1}, but not that of APC^{Cdc20}, was low, and the level of Cdh1 decreased 6 hr after DTB release of the infected cells, suggesting that APC^{Cdh1} undergoes unscheduled activation by *Shigella* (Figure 3E). This notion was also supported by WT *Shigella* (*dapB*$^{+}$) infection of HeLa cells, where the accumulation of Cyclin B1 in WT infection was greatly decreased compared with that of the noninfection control (Figure S4).

To demonstrate the activation of the APC^{Cdh1} upon WT infection, we investigated the polyubiquitination level of Cyclin B1 (Figure 4A, left). Approximately 9 hr after DTB release, which corresponded to the G2/M phase, APC^{Cdh1} was activated, with the APC interacting with Cdh1 as examined by immunoprecipitation with anti-APC3 antibody (Figure 4A, right). Indeed, when the level of APC^{Cdh1} activity upon WT infection was examined by measuring the half-lives of APC substrates such as Cdc20, Plk1, and Cyclin B1, the half-lives were decreased relative to that of Δ*ipaB* infection in either asynchronous (Figure 4B) or synchronous HeLa cells (Figures 4C).

IpaB and Mad2L2 Interaction Causes the Deregulation of APC^{Cdh1} Activity

To define the IpaB portion involved in Mad2L2 binding, we performed a yeast two-hybrid assay with various IpaB truncations and found that Mad2L2 shared a binding site with IpgC (IpaB chaperone) on IpaB: residues 61–70

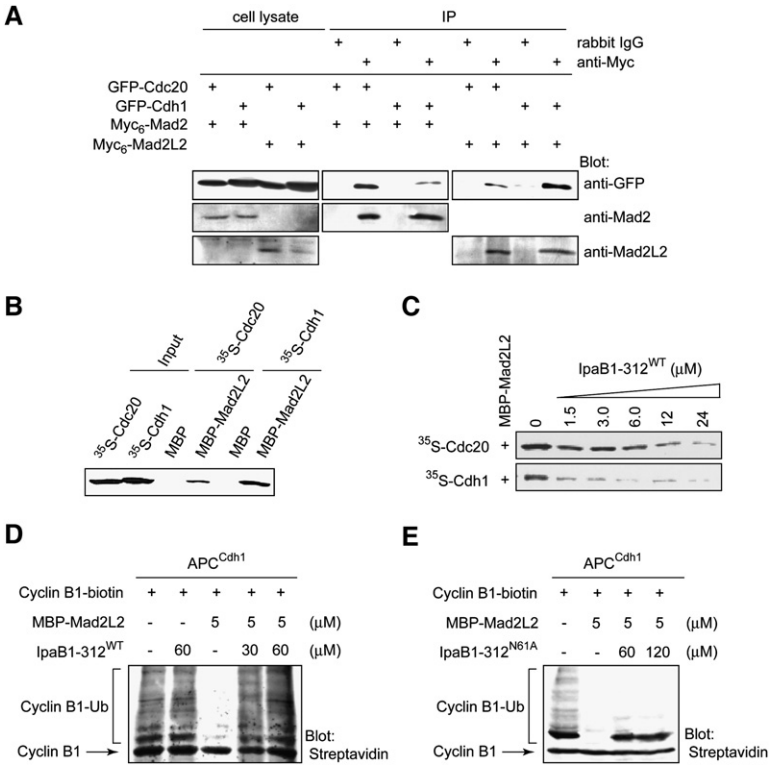

Figure 5. IpaB Suppresses Mad2L2 Inhibition of APC^{Cdh1}

(A) Mad2L2 bound Cdh1. 293T cells expressing GFP-Cdc20, GFP-Cdh1, Myc$_6$-Mad2, or Myc$_6$-Mad2L2 and treated with Colcemid 32 hr after transfection were lysed 16 hr later and immunoprecipitated with anti-Myc antibody or rabbit IgG and immunoblotted with anti-GFP, -Mad2, or -Mad2L2 antibodies.

(B) MBP-Mad2L2 bound to Cdc20 and Cdh1. MBP and MBP-Mad2L2 mixed with ^{35}S-Cdc20 or ^{35}S-Cdh1 were analyzed on a BAS2000.

(C) MBP-Mad2L2 binding to ^{35}S-Cdc20 or ^{35}S-Cdh1 is inhibited by IpaB1-312^{WT} in a dose-dependent manner.

(D) In vitro ubiquitination assays for purified APC in the presence or absence of MBP-Mad2L2 or/and IpaB1-312^{WT}. The APC was immunopurified from HeLa cell lysates and activated using recombinant Cdh1. The APC activated by Cdh1 was incubated with the N-terminal 100 residues of Cyclin B1-biotin.

(E) The same assay as in (D) but performed with IpaB1-312^{N61A}.

(Figure S5A). Because IpgC acts as the IpaB chaperone required for IpaB secretion via the TTSS (Page et al., 2001), we created Gal4 DBD-IpaB1-100 mutants that bound to AD-IpgC but not to AD-Mad2L2. An IpaB mutant unable to bind MBP-Mad2L2, N61A (IpaB1-312^{N61A}), was further investigated (Figures S5B and S5C). By narrowing down the portions of Mad2L2 used in IpaB-binding experiments, we found that residues 150–211 of Mad2L2 were involved in the interaction with IpaB (Figure S6).

To examine the interaction between Mad2L2 and Cdh1, we investigated 293T cells expressing GFP-Cdc20, GFP-Cdh1, Myc$_6$-Mad2, or Myc$_6$-Mad2L2 and found that more Cdh1 than Cdc20 was precipitated with Mad2L2 (Figure 5A). When ^{35}S-Cdc20 or ^{35}S-Cdh1 was mixed with MBP-Mad2L2, Cdh1 and Cdc20 were precipitated by MBP-Mad2L2, but not by MBP alone (Figure 5B). When ^{35}S-Cdc20 or ^{35}S-Cdh1 were pulled down after incubation with MBP-Mad2L2 in the presence of IpaB1-312^{WT} (at 1.5–24 μM), the amounts of ^{35}S-Cdc20 and ^{35}S-Cdh1 bound to MBP-Mad2L2 decreased as the amounts of IpaB1-312^{WT} increased (Figure 5C), suggesting that the IpaB/Mad2L2 interaction can activate APC^{Cdh1}. Indeed, polyubiquitination of Cyclin B1 by Cdh1-activated APC was almost completely blocked by MBP-Mad2L2, but the blockage was absent in the presence of IpaB1-312^{WT} (Figure 5D). Abrogation of Cyclin B1 polyubiquitination by MBP-Mad2L2 was not prevented by IpaB1-312^{N61A} (Figure 5E), adding further evidence that the IpaB/Mad2L2 interaction promotes unscheduled APC^{Cdh1} activation.

To confirm these findings, HeLa cells transfected with Mad2L2-RNAi 96 hr prior to synchronization in G1/S phase were re-transfected with Mad2L2-RNAi immediately after the first block, and the levels of Cdc20, Plk1, and Cyclin B1 were examined in cell lysates prepared between 0 and 15 hr after G1/S release (Figure S7). Although Luc-RNAi had no effect, Mad2L2 knockdown decreased the levels of Cdc20, Plk1, and Cyclin B1. The cellular levels of pHistone H3 were also decreased by Mad2L2-RNAi approximately 9 hr after DTB release (Figure S7A). In agreement with this, in Luc-RNAi-treated cells the peak of spherical cells occurred around 9 hr, opposed to a peak around 12 hr for the Mad2L2-RNAi-treated cells (Figure S7B). FACS analysis also showed that 12 hr after DTB release the population at G2/M phase was increased in cells transfected with Mad2L2-RNAi relative to those treated with Luc-RNAi (Figure S7C). Indeed, when pHistone H3-positive cells transfected with Mad2L2-RNAi were examined by immunostaining approximately 9 hr after DTB release, the percentage of positive cells was greatly diminished compared with that of cells transfected with the Luc-RNAi control (Figure S7D).

Involvement of the IpaB/Mad2L2 Interaction in Promoting Bacterial Colonization of the Intestinal Epithelium

To establish the physiological relevance of IpaB/Mad2L2 interaction to *Shigella*-directed cell-cycle arrest, we replaced the *ipaB* gene of YSH6000 with *ipaB*^{N61A} (*ipaB*::Km::*ipaB*^{N61A}) and *ipaB*^{WT} (*ipaB*::Km::*ipaB*^{WT}) and

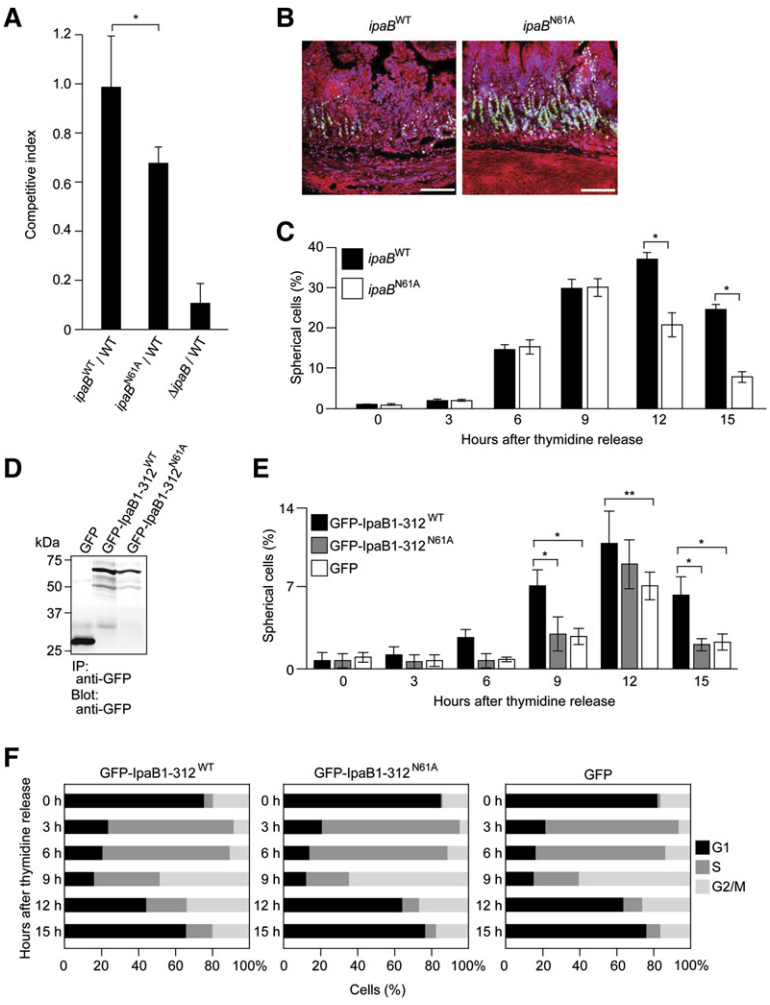

Figure 6. IpaB/Mad2L2-Dependent Cell-Cycle Arrest Is Exhibited during *Shigella* Infection

(A) The competitive index (1.0, no attenuation) is a measure of the ability of *ipaB*^{N61A} to colonize the rabbit ileal loops by comparing with WT. The competitive infections were carried out by the following combinations: WT/*ipaB*^{WT} (n = 12), WT/*ipaB*^{N61A} (n = 12), and WT/Δ*ipaB* (n = 6). *p < 0.05. Data are represented as mean ± SEM.

(B) Intestinal tissue immunostained with FITC-labeled anti-PCNA antibody (green) and counterstained with rhodamine-phalloidin (red) and TO-PRO3 (blue). Bars, 100 μm.

(C) Time course of transient spherical phenotype in synchronized HeLa cells after *ipaB*^{WT} or *ipaB*^{N61A} infection (moi 10). *p < 0.0001. Data are represented as mean ± SEM.

(D) Lysates of HeLa cells stably expressing GFP, GFP-IpaB1-312^{WT}, or GFP-IpaB1-312^{N61A} were immunoprecipitated with anti-GFP antibody and then immunoblotted with anti-GFP antibody.

(E) Time course of spherical cell occurrence among synchronized HeLa cells stably expressing GFP, GFP-IpaB1-312^{WT}, or GFP-IpaB1-312^{N61A}. *p < 0.0001. **p < 0.05. Data are represented as mean ± SEM.

(F) HeLa cells stably transfected with pEGFP, pEGFP-IpaB1-312^{WT}, or pEGFP-IpaB1-312^{N61A} were released from thymidine block at the times indicated. The cell-cycle stages of the cells were determined by FACS.

confirmed that their TTSS activity and invasiveness were similar (Figures S8A, S8B, and S8C). We also confirmed that the intracellular stabilities of IpaB and IpaB^{N61A} in synchronized HeLa cells were similar (Figure S8D). We then prepared a series of bacterial mixtures composed of equal numbers of YSH6000 (WT)/*ipaB*^{WT}, WT/*ipaB*^{N61A}, or WT/Δ*ipaB*, each of which were inoculated into rabbit intestinal ileal loops. Eighteen hours after inoculation, we measured bacterial numbers colonized per 0.5 cm^2 of intestinal tissues. Although WT and *ipaB*^{WT} colonized to a similar extent, *ipaB*^{N61A} showed less colonization (Figure 6A). Moreover, when 2 × 10^8 CFU of the strains were inoculated into different ileal loops, *ipaB*^{N61A} and *ipaB*^{WT}, but not YSH6200 (the noninvasive mutant), caused severe inflammatory responses accompanying *Shigella* invasion of the intestinal tissues 12 hr after inoculation (data not shown). Importantly, though PCNA-positive cells were rarely seen in the cryptic area after infection with *ipaB*^{WT}, many were observed after infection with *ipaB*^{N61A} (Figure 6B), indicating that the IpaB/Mad2L2 interaction is important for promoting *Shigella* infection. When HeLa cells synchronized by DTB release were infected by *Shigella* carrying *ipaB*^{WT} or *ipaB*^{N61A}, the percentage of spherical cells at 12 hr after release was lower with *ipaB*^{N61A} than with *ipaB*^{WT} (Figure 6C). Furthermore, when HeLa cells stably expressing GFP, GFP-IpaB1-312^{WT}, or GFP-IpaB1-312^{N61A} were synchronized to the G1/S phase by DTB, after release the percentage of spherical cells was higher among cells expressing GFP-IpaB1-312^{WT} than those expressing GFP-IpaB^{N61A} (Figure 6E). To confirm this, HeLa cells stably expressing GFP, GFP-IpaB1-312^{WT}, or GFP-IpaB1-312^{N61A} were synchronized in the G1/S phase by DTB, and after release, the cells that had incorporated bromodeoxyuridine (BrdU) into their nuclei were identified by anti-BrdU-FITC antibody (representing S phase cells) and propidium iodide (PI) staining (representing G1 and G2/M phase cells). Although the numbers of S- and G2/M-phased cells expressing GFP mock and GFP-IpaB1-312^{N61A} were similar, there were more such cells in cells expressing GFP-IpaB1-312^{WT} 12–15 hr after DTB release (Figure 6F). Thus, this series of experiments strongly suggested that the retardation of rapid intestinal epithelial renewal, due to the interaction of IpaB/Mad2L2 during *Shigella* infection, is pivotal to prolonging colonization within the intestinal epithelium.

DISCUSSION

In the present study, we have provided convincing in vitro and in vivo evidence that *Shigella* can modulate the cell-cycle progression of intestinal epithelial cells, and that the IpaB effector delivered via the TTSS into a host cell interacts with Mad2L2. This bacterial capability appears to affect epithelial cell turnover by slowing down cell renewal during infection, enabling *Shigella* to persist longer in its replicative niche.

The IpaB/Mad2L2 Interaction Activates APC^{Cdh1} at G2/M Phase

Mad2L2 was previously reported to be a Mad2-related protein capable of binding APC^{Cdh1} and inhibiting APC^{Cdh1} activation, though the precise role of Mad2L2 in modulating cell-cycle progression remains to be elucidated. Studies indicated that Mad2L2 plays a pivotal role in translesional DNA synthesis (TLS) in S phase cells (Cheung et al., 2006; Murakumo et al., 2006), and that it also participates in the spindle assembly checkpoint, similarly to Mad2 (Reimann et al., 2001b). In the present study, however, we did not observe GFP-IpaB1-312 within the nucleus in S phase HeLa cells, implying that IpaB is not involved in TLS. Since IpaB lacks a nuclear localization signal (NLS) and, at 62.2 kDa, is probably too large to enter the nucleus via passive diffusion, we speculate that its entry into the nucleus may occur by complex formation with Mad2L2, which does possess a putative NLS. Mad2L2 shares significant amino acid identity (25%) and similarity (48%) with Mad2 (Cahill et al., 1999). More recent studies have indicated that Mad2L2 can suppress the activation of APC^{Cdh1} (Pfleger et al., 2001). Emi1 is also known to suppress APC^{Cdh1} activation at G1/S phase, suggesting that Mad2L2 shows activity similar to Emi1 (Hsu et al., 2002). APC activation by Cdc20 is predominant at M phase, at which point the Mad2/Cdc20 interaction suppresses APC activation, while at M/G1 phase APC can be activated by Cdh1 (Peters, 2002). Mad2L2 is predominantly localized within the nuclei of BHK cells (Pfleger et al., 2001), and APC is also detected in the nuclei, suggesting that the Mad2L2 is able to influence APC activity at M/G1 phase. The activity of APC^{Cdh1} decreases at S phase (Bashir et al., 2004; Wei et al., 2004), at which point Emi1 participates in the inhibition of APC (Hsu et al., 2002), raising the possibility that Mad2L2 also takes part in activating APC at either S or G2/M phase. Therefore, using cell lysates prepared from HeLa cells synchronized at G1/S phase, we investigated whether Mad2L2 could control APC activity in M/G1, S, or G2/M phase. Our results of the immunoprecipitation assay with anti-Mad2L2 antibody clearly indicated that Mad2L2 does interact with APC in HeLa cells at G2/M phase (Figure S3B). Consistently, when GFP-IpaB1-312 and Myc$_6$-Mad2L2 were ectopically expressed in synchronized HeLa cells, both signals were detected within the nuclei at G2/M phase (Figure 2). Taken together, our results indicate that the IpaB/Mad2L2 interaction participates in the activation of APC^{Cdh1} at G2/M phase during *Shigella* infection.

Shigella Infection of Epithelial Cells Causes Cell-Cycle Arrest

The intestinal epithelium self-renews every few days, and its rapid turnover (including the tight sealing of epithelial cell-cell junctions) is the most important intrinsic host defense against bacterial colonization. The ability of *Shigella* IpaB to inhibit cell-cycle progression thus seems to be a bacterial strategy to prolong local persistence by blocking epithelial shedding. In addition, impairing the intestinal epithelial integrity, which also occurs as a consequence of cell-cycle progression inhibition (Nougayrede et al., 2005; Oswald et al., 2005), might further contribute to bacterial entry from the basolateral surface of epithelial cells, also promoting bacterial colonization. Because at its initial stages *Shigella* infection of intestinal epithelium takes place via the M cells, and the bacterial ability to slow cell-cycle progression was also anticipated to be less effective on well-differentiated superficial epithelial cells (Sansonetti, 2004), we pursued whether *Shigella* could directly access the intestinal cryptic area that is abundant in epithelial progenitors. Using a rabbit ileal loop infection model (Figure 3A) and a guinea pig rectal infection model (Shim et al., 2007), we have shown that *Shigella* infection can enter crypts and infect the cryptic epithelium by 12 hr post-infection (Figure 3A). At that stage, though we detected few epithelial progenitors after WT *Shigella* infection, epithelial progenitors remained abundant after infection with the *ipaB* mutant (Figure 3B). Likewise, the ability of *Shigella* to induce cell-cycle arrest could be reproduced using synchronized HeLa cells infected with WT but not *ipaB* mutant bacteria (Figure 3D). WT *Shigella* infection of HeLa cells generated more spherical cells with condensed chromatin than did the *ipaB* mutant 6 hr after G1/S release; furthermore, the spherical cells were TUNEL negative, implying that the spherical cells were not a consequence of apoptosis. Indeed, because the spherical HeLa cells caused by *Shigella* infection showed poor spindle formation, we assumed that the cell-cycle arrest caused in the infected HeLa cells occurred prior to metaphase. Thus our data indicate that IpaB plays an important role in causing cell-cycle arrest, although we have not excluded the possibility that other *Shigella* proteins might also play a role in affecting cell-cycle progression.

Shigella Infection of Epithelial Cells Preferentially Activates APC^{Cdh1}

If the activation of APC in HeLa cells truly occurred as a consequence of the IpaB/Mad2L2 interaction during *Shigella* infection, one would anticipate that the degradation of APC^{Cdh1} substrates would also take place. We therefore investigated the levels of Cyclin B1, Cdc20, and Plk1, known substrates for APC^{Cdh1} and, to a lesser extent, for APC^{Cdc20}. Indeed, the levels of Cyclin B1, Cdc20, and Plk1 in HeLa cells 9 hr after G1/S release underwent degradation after infecting with WT but not with

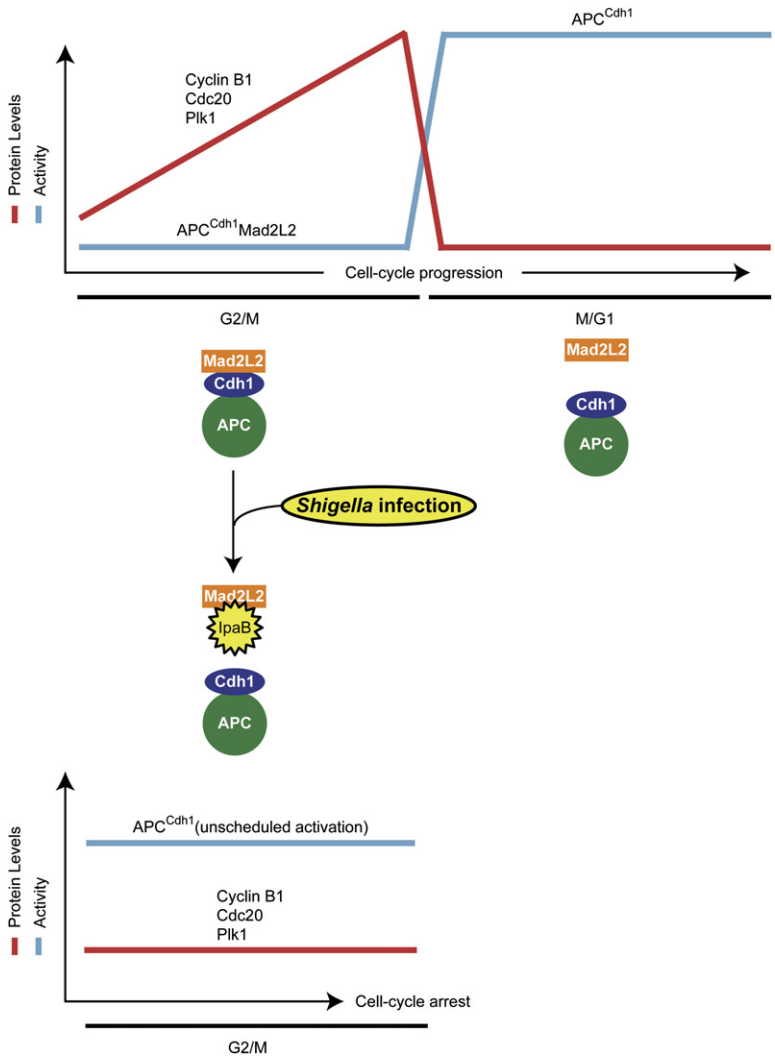

Figure 7. Proposed Model of the Role of IpaB in Cell-Cycle Progression Interference

Mad2L2 interaction with APC^{Cdh1} increases during G2/M (Figure S3B) and could therefore result in the accumulation of Cyclin B1, Cdc20, and Plk1 in G2/M (Figure S7A). Unscheduled activation of APC^{Cdh1} in G2/M by IpaB (Figure 3E) could explain the mitotic abnormalities in *Shigella*-infected cells (Figure 3D) and, in turn, leads to premature degradation of Cyclin B1, Cdc20, and Plk1, a delay in mitotic progression, and faulty mitosis.

the *ipaB* mutant *Shigella* (Figure 3E). As Cdc20 and Plk1 are substrates for APC^{Cdh1} but not APC^{Cdc20} (Castro et al., 2005), the above results suggest that APC^{Cdh1} activation, but not that of APC^{Cdc20}, occurred as the *Shigella*-induced unscheduled activation. In this regard, it is worth noting that *Shigella* infection had a smaller effect on the levels of Cyclin A than those of Cyclin B1, Cdc20, or Plk1 (Figure 3E). The fact that Cyclin A is an APC^{Cdh1} substrate, and its rate of degradation is slower than that of other APC^{Cdh1} substrates (Rape et al., 2006), may explain *Shigella* infection's smaller effect on Cyclin A degradation than on the other APC^{Cdh1} substrates. In any case, our results strongly indicate that an unscheduled activation of APC^{Cdh1} takes place in HeLa cells at G2/M phase following *Shigella* infection (Figure 4).

In addition to the activation of APC by Cdc20 and Cdh1, the activation of APC is also accompanied by phosphorylation of APC3 (Kraft et al., 2003), an APC subunit, by other host factors. Knockout or -down of Mad2 causes early sister chromatid segregation in the presence of spindle formation inhibitor (Michel et al., 2001, 2004; De Antoni et al., 2005; Luo et al., 2004). In contrast, knockdown of Mad2L2 results in a delay in cell-cycle progression (see Figure S7C). Although Mad2 also contributes to a delay in cell-cycle progression, Mad2L2 can promote cell cycling as do APC inhibitors such as Emi1 and RASSF1A (Hsu et al., 2002; Song et al., 2004). Importantly, upon *Shigella* infection of HeLa cells, the phosphorylation of APC3 was also detected, though the result was not dramatic (Figure 3E). Although we do not understand how APC3 phosphorylation is stimulated by *Shigella* infection, because the levels of Cyclin B1 and Plk1 were greatly decreased, the upregulation of phosphorylated APC3 does not seem to be mediated by Cyclin B1-dependent or Plk1 kinase; rather, other uncharacterized factor(s) may be involved in the phosphorylation of APC3. In HeLa cells infected with WT but not with *ipaB* mutant *Shigella*, the levels of Cdh1 were also remarkably decreased (Figure 3E). As Cdh1 has been shown to undergo degradation by APC^{Cdh1} at G0 or G1 phase (Listovsky et al.,

2004), the decrease in Cdh1 after *Shigella* infection is also consistent with bacterial infection-induced unscheduled activation of APC^{Cdh1}.

How Does Host Cell-Cycle Arrest by *Shigella* Contribute to Bacterial Colonization?

The present study demonstrates that the cell-cycle progression modulated by APC's ubiquitin ligase activity can be slowed by the delivery of IpaB by *Shigella* into the host cells. How does this activity contribute to the bacterial colonization of the intestinal epithelium? As noted above, as the rapid turnover of epithelial layers limits bacterial colonization, it is possible that slowing this turnover could prolong *Shigella*'s replicative foothold. Although the situation is different than with *Shigella*, a similar hypothesis was recently postulated for *Trichuris trichuria*, a cecal-dwelling parasitic nematode. In the case of *Trichuris*, an increase in the rate of epithelial cell turnover in murine large intestines acted as an "epithelial escalator" to efficiently expel *Trichuris* (Cliffe et al., 2005). To investigate this idea, we created $IpaB^{N61A}$, a single amino acid-substituted IpaB mutant, which interacts more weakly with Mad2L2 (Figure S5) but still functions as a TTSS translocator (Figures S8A and S8B) and supports bacterial invasion of epithelial cells (Figure S8C). We compared this mutant's ability to deregulate APC activity via Mad2L2 to that of WT IpaB in a Cyclin B1 ubiquitination assay. The results clearly showed that the inhibition of APC^{Cdh1} by Mad2L2, as examined by the Cyclin B1 ubiquitination level, was reduced by the addition of IpaB but not $IpaB^{N61A}$ into the assay medium (Figures 5D and 5E). Importantly, when a bacteria mixture composed of an equal number of *Shigella* expressing IpaB and *Shigella* expressing $IpaB^{N61A}$ was inoculated into rabbit ileal loops, the colonization rate of *Shigella* expressing IpaB was much more efficient than that of *Shigella* expressing $IpaB^{N61A}$ (Figure 6A), further supporting the idea that the IpaB/Mad2L2 interaction is functionally important for bacterial colonization. In further support of our hypothesis, it has become increasingly evident that certain cyclomodulins, bacterial toxins, and effectors that modulate the eukaryotic cell cycle can target epithelial cells and control their cell-cycle progression (Nougayrede et al., 2005; Oswald et al., 2005). For example, Cytolethal-distending toxin (CDT), which is produced by a group of unrelated Gram-negative pathogenic bacteria, causes cell-cycle arrest in epithelial cells, though the targeted phase of the cell cycle varies between cell types (Lara-Tejero and Galan, 2000; Whitehouse et al., 1998). In these studies, the ability of CDT to cause cell-cycle arrest raises the possibility that prolonging local bacterial existence can be achieved by slowing epithelial renewal.

In summary, our study has provided convincing evidence that *Shigella* influence epithelial cell-cycle progression by delivering IpaB into host cells. Once inside, IpaB interferes with the binding of Mad2L2 to Cdh1, leading to unscheduled activation of APC and subsequent Cyclin B1 degradation (Figure 7). We conclude that the retardation of intestinal epithelial renewal during *Shigella* infection prolongs bacterial colonization of the intestinal epithelium. To our knowledge, this is the first evidence that a bacterial TTSS-mediated effector, IpaB, targets epithelial cells and directly modulates their cell-cycle progression by targeting the activity of APC.

EXPERIMENTAL PROCEDURES

Yeast Two-Hybrid Assay

The yeast two-hybrid screen was performed with the Matchmaker GAL4 Two-Hybrid System 3 (Clontech), AH109 cotransformed with pGBKT7-*ipaB1-936*, a GAL4 DNA-binding domain vector, and a HeLa cDNA library cloned into a GAL4 activation domain vector, pACT2.

Pull-Down Assays

GST-Mad2L2 bound to glutathione sepharose 4B was mixed with recombinant IpaB for 2 hr at 4°C. After centrifugation, the beads were washed three times with 1% Triton X-100-PBS and immunoblotted. The MBP-Mad2L2 bound to the amylose resin was mixed with recombinant IpaB derivatives or ^{35}S-labeled proteins and incubated for 2 hr at 4°C. Following centrifugation, the supernatant was discarded and the beads were subjected to immunoblotting after washing with 0.1% Tween 20-PBS eight times.

Coimmunoprecipitations

In our endogenous coimmunoprecipitation experiments, HeLa lysates were spun at 15,000 rpm for 15 min at 4°C. After adding 2 μg of primary antibody (anti-Mad2, -APC3, or -Mad2L2 antibodies)-protein G-sepharose complex to the lysates, they were placed on ice for 2 hr. Mouse IgG was used as a negative control. Immunoprecipitates were washed three times with lysis buffer and then subjected to immunoblotting.

Cell Synchronization

HeLa G1/S cells were prepared by double thymidine block (DTB). The cells were first arrested with 2.0 mM thymidine for 20 hr, released into thymidine-free medium for 8 hr, and arrested again by incubation in 2.0 mM thymidine for 16 hr. Synchronous mitotic cells were obtained by incubating for 16 hr in medium containing Colcemid (Demecolcine, Sigma) at 150 ng/ml.

RNAi

A small interfering RNA (CAGAAACGCAAGAAGUACA) duplex specific for Mad2L2 repression was transfected into cells using Oligofectamine (Invitrogen), according to the manufacturer's instructions.

Immunohistochemical Staining for PCNA

To identify PCNA-positive crypt cells in the rabbit intestine, tissue specimens fixed with 4% paraformaldehyde in PBS were frozen in liquid nitrogen and sectioned by a Leica cryostat (model CM 1900). The sections were fixed for 4 min in acetone at 4°C and then air-dried at room temperature. Sections were prepared and placed in 10 mM sodium citrate buffer (pH 6.0), which was brought to a boil in a microwave oven, and the sections were allowed to cool to room temperature. The tissue was neutralized by two rinses in PBS-0.5% Tween 20 (PBS-T). The sections were blocked for 30 min with PBS (pH 7.4) containing 10% goat serum and incubated with primary antibody (anti-PCNA, PC10) at a dilution of 1:100 in the above medium for 60 min. The sections were then rinsed in PBS-T and incubated with secondary antibody (anti-mouse IgG-FITC, 1:100) for 60 min.

Ubiquitination Assay

The ubiquitination assay was carried out as previously described (Kotani et al., 1998). The N terminus of human Cyclin B1 cDNA, encoding

amino acid residues 1–100, was inserted into the BamHI-XhoI site of pET21a or NdeI site of pET42a and expressed in BL21 cells. The His-tagged recombinant Cyclin B1 protein was purified and biotinylated using a kit (Pierce). The purified APC was mixed in 30 μl of 10 mM Tris (pH 7.6), 0.5 mM $MgCl_2$, 1.5 mM DTT, 10 mM ATP, 5 μg recombinant E1, 1 μg/ml recombinant E2hC, 1 μg/ml recombinant E2H5B, 20 μg/ml ubiquitin (Sigma), 1 μg/ml recombinant Cdh1, and 10 μg/ml biotinylated Cyclin B1 and then incubated at 25°C for 30 min.

Competitive Colonization Assay

Rabbit ileal loops were inoculated with 0.5 ml of a mixture (approximately 1:1) of WT (Km^S) and *ipaB* mutant (Km^R) *Shigella* (total inoculum, 4×10^8 CFU in PBS), and each loop was treated twice with PBS containing 50 μg/ml gentamicin. Similar-sized tissue specimens obtained with an 8 mm diameter biopsy punch were washed with PBS to eliminate residual gentamicin. The tissue samples were then ground in ice-cold PBS, and a 1/10 dilution was prepared in tryptic soy broth (TCS) and incubated for 30 min at 37°C with aeration. Serial dilutions of this culture were then plated on agar and incubated overnight at 37°C. CFUs were counted and the number of bacteria was calculated per 0.5 cm^2 of intestinal tissue.

Flow Cytometry

Cell-cycle distribution was determined by propidium iodide (PI) or PI/BrdU double staining. For PI/BrdU double staining, BrdU was added to the culture medium 30 min prior to harvesting. BrdU incorporation was detected with a FITC-labeled mouse anti-BrdU antibody, and both DNA content and BrdU incorporation were analyzed by a FACSCalibur flow cytometer.

Statistical Analysis

Values are reported as means ± standard error of the mean. p values were calculated by using a nonparametric one-tailed Mann-Whitney *U*-test.

Supplemental Data

Supplemental Data include Experimental Procedures, eight figures, and Supplemental References and are available with this article online at http://www.cell.com/cgi/content/full/130/4/611/DC1/.

ACKNOWLEDGMENTS

We thank the members of the Sasakawa Laboratory, especially T. Suzuki, S. Yoshida, and M. Fukumatsu, for their helpful advice. We are grateful to R.F. Whittier for critical reading of the manuscript. This work was supported by a Grant-in-Aid for the Scientific Research on Priority Areas from the Ministry of Education, Culture, Sports, Science and Technology of Japan (MEXT) and the Special Coordination Funds for Promoting Science from Japan Science and Technology Agency (JSTA). M.K. is the recipient of the Japan Society for the Promotion of Science (JSPS) postdoctoral fellowship for a foreign researcher. P.K.J. is an employee of Genentech, Inc.

Received: August 30, 2006
Revised: March 29, 2007
Accepted: June 21, 2007
Published: August 23, 2007

REFERENCES

Bashir, T., Dorrello, N.V., Amador, V., Guardavaccaro, D., and Pagano, M. (2004). Control of the SCF(Skp2-Cks1) ubiquitin ligase by the APC/C(Cdh1) ubiquitin ligase. Nature *428*, 190–193.

Blocker, A., Gounon, P., Larquet, E., Niebuhr, K., Cabiaux, V., Parsot, C., and Sansonetti, P. (1999). The tripartite type III secreton of *Shigella flexneri* inserts IpaB and IpaC into host membranes. J. Cell Biol. *147*, 683–693.

Cahill, D.P., da Costa, L.T., Carson-Walter, E.B., Kinzler, K.W., Vogelstein, B., and Lengauer, C. (1999). Characterization of MAD2B and other mitotic spindle checkpoint genes. Genomics *58*, 181–187.

Castro, A., Bernis, C., Vigneron, S., Labbe, J.C., and Lorca, T. (2005). The anaphase-promoting complex: a key factor in the regulation of cell cycle. Oncogene *24*, 314–325.

Chen, J., and Fang, G. (2001). MAD2B is an inhibitor of the anaphase-promoting complex. Genes Dev. *15*, 1765–1770.

Chen, Y., Smith, M.R., Thirumalai, K., and Zychlinsky, A. (1996). A bacterial invasin induces macrophage apoptosis by binding directly to ICE. EMBO J. *15*, 3853–3860.

Cheung, H.W., Chun, A.C., Wang, Q., Deng, W., Hu, L., Guan, X.Y., Nicholls, J.M., Ling, M.T., Chuan Wong, Y., Tsao, S.W., et al. (2006). Inactivation of human MAD2B in nasopharyngeal carcinoma cells leads to chemosensitization to DNA-damaging agents. Cancer Res. *66*, 4357–4367.

Cliffe, L.J., Humphreys, N.E., Lane, T.E., Potten, C.S., Booth, C., and Grencis, R.K. (2005). Accelerated intestinal epithelial cell turnover: a new mechanism of parasite expulsion. Science *308*, 1463–1465.

Cossart, P., and Sansonetti, P.J. (2004). Bacterial invasion: the paradigms of enteroinvasive pathogens. Science *304*, 242–248.

De Antoni, A., Pearson, C.G., Cimini, D., Canman, J.C., Sala, V., Nezi, L., Mapelli, M., Sironi, L., Faretta, M., Salmon, E.D., and Musacchio, A. (2005). The Mad1/Mad2 complex as a template for Mad2 activation in the spindle assembly checkpoint. Curr. Biol. *15*, 214–225.

Fang, G., Yu, H., and Kirschner, M.W. (1998). The checkpoint protein MAD2 and the mitotic regulator CDC20 form a ternary complex with the anaphase-promoting complex to control anaphase initiation. Genes Dev. *12*, 1871–1883.

Habu, T., Kim, S.H., Weinstein, J., and Matsumoto, T. (2002). Identification of a MAD2-binding protein, CMT2, and its role in mitosis. EMBO J. *21*, 6419–6428.

Hilbi, H., Moss, J.E., Hersh, D., Chen, Y., Arondel, J., Banerjee, S., Flavell, R.A., Yuan, J., Sansonetti, P.J., and Zychlinsky, A. (1998). *Shigella*-induced apoptosis is dependent on caspase-1 which binds to IpaB. J. Biol. Chem. *273*, 32895–32900.

Hsu, J.Y., Reimann, J.D., Sorensen, C.S., Lukas, J., and Jackson, P.K. (2002). E2F-dependent accumulation of hEmi1 regulates S phase entry by inhibiting APC(Cdh1). Nat. Cell Biol. *4*, 358–366.

Kotani, S., Tugendreich, S., Fujii, M., Jorgensen, P.M., Watanabe, N., Hoog, C., Hieter, P., and Todokoro, K. (1998). PKA and MPF-activated polo-like kinase regulate anaphase-promoting complex activity and mitosis progression. Mol. Cell *1*, 371–380.

Kraft, C., Herzog, F., Gieffers, C., Mechtler, K., Hagting, A., Pines, J., and Peters, J.M. (2003). Mitotic regulation of the human anaphase-promoting complex by phosphorylation. EMBO J. *22*, 6598–6609.

Lafont, F., Tran Van Nhieu, G., Hanada, K., Sansonetti, P., and van der Goot, F.G. (2002). Initial steps of *Shigella* infection depend on the cholesterol/sphingolipid raft-mediated CD44-IpaB interaction. EMBO J. *21*, 4449–4457.

Lara-Tejero, M., and Galan, J.E. (2000). A bacterial toxin that controls cell cycle progression as a deoxyribonuclease I-like protein. Science *290*, 354–357.

Lara-Tejero, M., and Galan, J.E. (2002). Cytolethal distending toxin: limited damage as a strategy to modulate cellular functions. Trends Microbiol. *10*, 147–152.

Listovsky, T., Oren, Y.S., Yudkovsky, Y., Mahbubani, H.M., Weiss, A.M., Lebendiker, M., and Brandeis, M. (2004). Mammalian Cdh1/Fzr mediates its own degradation. EMBO J. *23*, 1619–1626.

Luo, X., Tang, Z., Xia, G., Wassmann, K., Matsumoto, T., Rizo, J., and Yu, H. (2004). The Mad2 spindle checkpoint protein has two distinct natively folded states. Nat. Struct. Mol. Biol. *11*, 338–345.

Marches, O., Ledger, T.N., Boury, M., Ohara, M., Tu, X., Goffaux, F., Mainil, J., Rosenshine, I., Sugai, M., De Rycke, J., and Oswald, E. (2003). Enteropathogenic and enterohaemorrhagic *Escherichia coli* deliver a novel effector called Cif, which blocks cell cycle G2/M transition. Mol. Microbiol. *50*, 1553–1567.

Michel, L., Diaz-Rodriguez, E., Narayan, G., Hernando, E., Murty, V.V., and Benezra, R. (2004). Complete loss of the tumor suppressor MAD2 causes premature Cyclin B degradation and mitotic failure in human somatic cells. Proc. Natl. Acad. Sci. USA *101*, 4459–4464.

Michel, L.S., Liberal, V., Chatterjee, A., Kirchwegger, R., Pasche, B., Gerald, W., Dobles, M., Sorger, P.K., Murty, V.V., and Benezra, R. (2001). MAD2 haplo-insufficiency causes premature anaphase and chromosome instability in mammalian cells. Nature *409*, 355–359.

Murakumo, Y., Mizutani, S., Yamaguchi, M., Ichihara, M., and Takahashi, M. (2006). Analyses of ultraviolet-induced focus formation of hREV1 protein. Genes Cells *11*, 193–205.

Nasmyth, K. (2005). How do so few control so many? Cell *120*, 739–746.

Nougayrede, J.P., Taieb, F., De Rycke, J., and Oswald, E. (2005). Cyclomodulins: bacterial effectors that modulate the eukaryotic cell cycle. Trends Microbiol. *13*, 103–110.

Ogawa, M., and Sasakawa, C. (2006). Intracellular survival of *Shigella*. Cell. Microbiol. *8*, 177–184.

Oswald, E., Nougayrede, J.P., Taieb, F., and Sugai, M. (2005). Bacterial toxins that modulate host cell-cycle progression. Curr. Opin. Microbiol. *8*, 83–91.

Page, A.L., Fromont-Racine, M., Sansonetti, P., Legrain, P., and Parsot, C. (2001). Characterization of the interaction partners of secreted proteins and chaperones of *Shigella flexneri*. Mol. Microbiol. *42*, 1133–1145.

Parsot, C. (2005). *Shigella* spp. and enteroinvasive *Escherichia coli* pathogenicity factors. FEMS Microbiol. Lett. *252*, 11–18.

Peters, J.M. (2002). The anaphase-promoting complex: proteolysis in mitosis and beyond. Mol. Cell *9*, 931–943.

Pfleger, C.M., Salic, A., Lee, E., and Kirschner, M.W. (2001). Inhibition of Cdh1-APC by the MAD2-related protein MAD2L2: a novel mechanism for regulating Cdh1. Genes Dev. *15*, 1759–1764.

Philpott, D.J., Yamaoka, S., Israel, A., and Sansonetti, P.J. (2000). Invasive *Shigella flexneri* activates NF-kappa B through a lipopolysaccharide-dependent innate intracellular response and leads to IL-8 expression in epithelial cells. J. Immunol. *165*, 903–914.

Potten, C.S. (1998). Stem cells in gastrointestinal epithelium: numbers, characteristics and death. Philos. Trans. R. Soc. Lond. B Biol. Sci. *353*, 821–830.

Rape, M., Reddy, S.K., and Kirschner, M.W. (2006). The processivity of multiubiquitination by the APC determines the order of substrate degradation. Cell *124*, 89–103.

Reimann, J.D., Freed, E., Hsu, J.Y., Kramer, E.R., Peters, J.M., and Jackson, P.K. (2001a). Emi1 is a mitotic regulator that interacts with Cdc20 and inhibits the anaphase promoting complex. Cell *105*, 645–655.

Reimann, J.D., Gardner, B.E., Margottin-Goguet, F., and Jackson, P.K. (2001b). Emi1 regulates the anaphase-promoting complex by a different mechanism than Mad2 proteins. Genes Dev. *15*, 3278–3285.

Sansonetti, P.J. (2004). War and peace at mucosal surfaces. Nat. Rev. Immunol. *4*, 953–964.

Shim, D.H., Suzuki, T., Chang, S.Y., Park, S.M., Sansonetti, P.J., Sasakawa, C., and Kweon, M.N. (2007). New animal model of shigellosis in the Guinea pig: its usefulness for protective efficacy studies. J. Immunol. *178*, 2476–2482.

Song, M.S., Song, S.J., Ayad, N.G., Chang, J.S., Lee, J.H., Hong, H.K., Lee, H., Choi, N., Kim, J., Kim, H., et al. (2004). The tumour suppressor RASSF1A regulates mitosis by inhibiting the APC-Cdc20 complex. Nat. Cell Biol. *6*, 129–137.

Tang, Z., Bharadwaj, R., Li, B., and Yu, H. (2001). Mad2-Independent inhibition of APCCdc20 by the mitotic checkpoint protein BubR1. Dev. Cell *1*, 227–237.

Vodermaier, H.C. (2004). APC/C and SCF: controlling each other and the cell cycle. Curr. Biol. *14*, R787–R796.

Wei, W., Ayad, N.G., Wan, Y., Zhang, G.J., Kirschner, M.W., and Kaelin, W.G., Jr. (2004). Degradation of the SCF component Skp2 in cell-cycle phase G1 by the anaphase-promoting complex. Nature *428*, 194–198.

Whitehouse, C.A., Balbo, P.B., Pesci, E.C., Cottle, D.L., Mirabito, P.M., and Pickett, C.L. (1998). *Campylobacter jejuni* cytolethal distending toxin causes a G2-phase cell cycle block. Infect. Immun. *66*, 1934–1940.

Xia, G., Luo, X., Habu, T., Rizo, J., Matsumoto, T., and Yu, H. (2004). Conformation-specific binding of p31(comet) antagonizes the function of Mad2 in the spindle checkpoint. EMBO J. *23*, 3133–3143.

Zychlinsky, A., Prevost, M.C., and Sansonetti, P.J. (1992). *Shigella flexneri* induces apoptosis in infected macrophages. Nature *358*, 167–169.